nature medicine

BRIEF COMMUNICATIONS

Functional and morphological recovery of dystrophic muscles in mice treated with deacetylase inhibitors

G C Minetti[1,9], C Colussi[2,9], R Adami[3,9], C Serra[1,4], C Mozzetta[1], V Parente[3], S Fortuni[1], S Straino[2], M Sampaolesi[5], M Di Padova[6], B Illi[7], P Gallinari[8], C Steinkühler[8], M C Capogrossi[2], V Sartorelli[6], R Bottinelli[3], C Gaetano[2] & P L Puri[1,4]

Pharmacological interventions that increase myofiber size counter the functional decline of dystrophic muscles[1,2]. We show that deacetylase inhibitors increase the size of myofibers in dystrophin-deficient (MDX) and α-sarcoglycan (α-SG)–deficient mice by inducing the expression of the myostatin antagonist follistatin[3] in satellite cells. Deacetylase inhibitor treatment conferred on dystrophic muscles resistance to contraction-coupled degeneration and alleviated both morphological and functional consequences of the primary genetic defect. These results provide a rationale for using deacetylase inhibitors in the pharmacological therapy of muscular dystrophies.

Enlarging fiber size in dystrophic muscles produces beneficial effects in dystrophin-deficient MDX mice, a model of Duchenne muscular dystrophy (DMD)[2,4–6]. Previous studies have shown that three structurally unrelated deacetylase inhibitors—trichostatin A (TSA), valproic acid (VPA) and phenylbutyrate (PhB)—share the ability to promote myoblast fusion into hypernucleated myotubes with an increased size relative to myotubes formed in the absence of drugs[7,8]. To select a compound for long-term treatment of dystrophic mice, we compared the results of pilot experiments in which MDX mice were exposed to TSA (0.6 mg per kg body weight per day), VPA (160 mg/kg per day) or PhB (90 mg/kg per day) by daily intraperitoneal injections. We chose to begin the treatment when the first manifestations of the disease were already evident, as we sought to evaluate the efficacy of deacetylase inhibitors in a situation simulating the clinical stage at which human patients typically receive the diagnosis of muscular dystrophy[9]. Increased histone acetylation, which reflects the bioactivity of deacetylase inhibitors, was detected in muscles and other peripheral organs (for example, brain) a few hours after injection, indicating rapid uptake of the compounds (**Supplementary Figure 1** online). We next evaluated the ability of satellite cells from MDX mice exposed to the deacetylase inhibitors for 10 d to differentiate into multinucleated myotubes. After 24 h in differentiation medium, myotubes were present only in cultures of satellite cells isolated from mice exposed to deacetylase inhibitors (**Supplementary Figure 2** online). Notably, satellite cells derived from TSA-treated mice formed myotubes with the highest efficiency and showed an increased expression, relative to that in untreated controls, of myosin heavy chain (MyHC)—a marker of terminal differentiation—and of regeneration markers, such as follistatin and embryonic and perinatal MyHC (**Supplementary Figure 2**). Only satellite cells from TSA-treated mice showed reduced levels of myostatin mRNA relative to those from untreated controls. Treatment of 12-week-old mice with deacetylase inhibitors for an additional three months prevented an increase in serum concentrations of creatine kinase, a biomarker for the severity of the disease (**Supplementary Figure 2**). The decline of creatine kinase concentrations was more pronounced in mice exposed to TSA.

Among the three compounds, TSA was the best tolerated for long-term treatment and did not cause noticeable side effect or signs of toxicity, such as body weight reduction, hyperexcitability or sudden death. By contrast, we observed an increased incidence of mortality in VPA- and PhB-treated mice. These results encouraged us to select TSA for extensive analysis of the effect of prolonged exposure of dystrophic mice to deacetylase inhibitors.

We first administered TSA to MDX mice for 3 months, starting at 12 weeks of age, and investigated its effects on force production by dystrophic muscles *in vitro* and on exercise performance *in vivo*. We isolated the extensor digitorum longus (EDL) muscles from MDX mice previously exposed to either TSA or control vehicle, and we compared the force they generated to that generated by EDL from normal mice. EDL from MDX mice developed less force during tetanic contraction, and treatment with TSA restored EDL force in MDX mice to values comparable to those from normal muscles (**Fig. 1a**). At the end of the test, we investigated the integrity of the sarcolemma of EDL postcontraction by evaluating the uptake of Evans blue dye, which was higher in MDX muscles than in normal muscles (**Fig. 1b**). EDL from TSA-treated MDX mice showed less uptake than EDL from untreated MDX mice (**Fig. 1b**). We next determined whether the increase in muscle strength *in vitro* correlated with increased whole-body strength in TSA-treated MDX mice *in vivo*. Six-month-old MDX mice showed a significantly shorter time to exhaustion in the treadmill test than did normal mice. TSA-treated

[1]Dulbecco Telethon Institute at Fondazione A. Cesalpino, Institute of Cell Biology and Tissue Engineering, San Raffaele Biomedical Science Park of Rome, Via Castel Romano 100, 00128, Rome, Italy. [2]Istituto Dermopatico dell'Immacolata, Istituto di Ricovero e Cura a Carattere Scientifico (IRCCS) Laboratory of Vascular Pathology, Via Monti dei Creta 104, 00167, Rome, Italy. [3]Department of Experimental Medicine, Human Physiology Unit and Interuniversity Institute of Myology, University of Pavia, Via Forlanini 6, 27100, Pavia, Italy. [4]The Burnham Institute, 10010 N. Torrey Pines Road, La Jolla, California 92037, USA. [5]Stem Cell Research Institute, H. S. Raffaele, Via Olgettina 58, 20132, Milan, Italy. [6]Muscle Gene Expression Group, Laboratory of Muscle Biology, National Institute of Arthritis and Musculoskeletal and Skin Diseases, National Institutes of Health, 50 South Drive, Bethesda, Maryland 20892, USA. [7]Laboratory of Vascular Biology and Gene Therapy, Centro Cardiologico Monzino, IRCCS, Via Parea 4, 20138, Milan, Italy. [8]Istituto di Ricerche di Biologia Molecolare P. Angeletti, Via Pontina Km 30600, 00040, Rome, Italy. [9]These authors contributed equally to this work. Correspondence should be addressed to P.L.P. (plpuri@dti.telethon.it or lpuri@burnham.org).

Received 27 January; accepted 8 August; published online 17 September 2006; doi:10.1038/nm1479

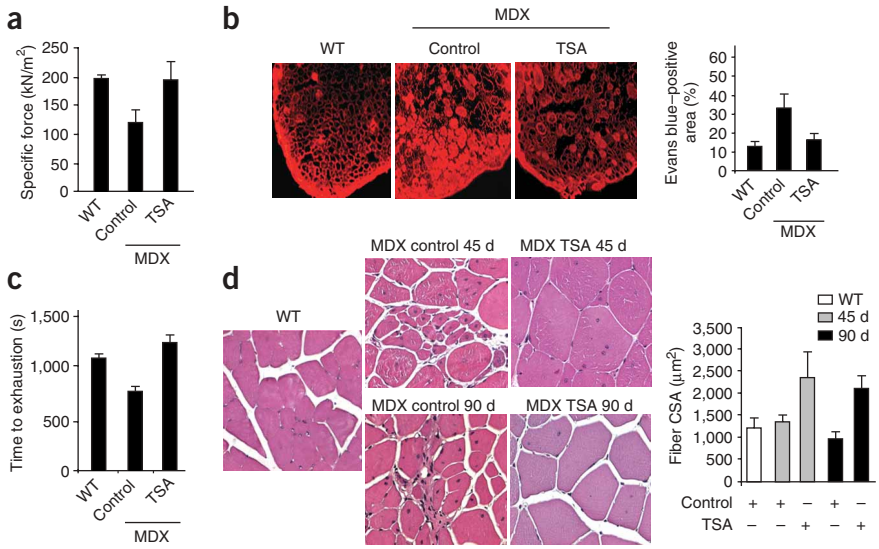

Figure 1 TSA treatment restores muscle function and morphology in MDX mice. (**a**) EDL muscles isolated from C57BL/10 wild-type (WT; $n = 8$) and MDX control untreated (control; $n = 10$) or TSA-treated ($n = 8$) mice were electrically stimulated *in vitro* to elicit force of fused tetani (P_0), which was expressed relative to CSA (P_0/CSA, force per square meter (kN/m^2)). P_0/CSA of EDL muscles was significantly lower ($P = 0.0009$) in MDX mice and recovered to normal values in TSA-treated mice (MDX control versus MDX TSA treated $P = 0.026$). (**b**) Evans blue uptake in EDL muscles after the force test, scored as percentage Evans blue–positive area. Original magnification, ×5. (**c**) Treadmill test. MDX control untreated mice ($n = 10$) showed a significantly poorer performance ($P = 0.0001$) than WT mice ($n = 10$). TSA-treated mice ($n = 8$) recovered to normal values (control MDX versus TSA-treated MDX $P = 0.0017$). (**d**) H&E staining of adductor from control untreated ($n = 4$) and TSA-treated ($n = 4$) MDX mice at 45 and 90 d of treatment. TSA induced a significant increase in fiber CSA at both 45 and 90 d for all the muscles treated with TSA ($P < 0.001$). Original magnification, ×40.

MDX mice showed a full recovery of exercise performance (**Fig. 1c**). A similar recovery of exercise performance in TSA-treated MDX mice was observed in a swimming test (**Supplementary Figure 3** online).

Deacetylase inhibitors typically increase gene transcription by promoting histone hyperacetylation. Utrophin, a functional analog of dystrophin, is upregulated in dystrophic muscles from humans with muscular dystrophy and in MDX mice. A further increase in utrophin levels is reported to provide beneficial effect in dystrophic muscles[10]. However, TSA treatment did not increase utrophin levels in the myofibers of treated MDX mice, nor could we detect dystrophin in muscles from TSA-treated mice (**Supplementary Figure 3**).

Histological evaluation of skeletal muscles from TSA-treated MDX mice revealed a progressive increase in the size of myofibers from all the muscles analyzed (**Fig. 1d** shows the adductor as representative). The fiber cross-sectional area (CSA) of the muscles isolated from treated MDX mice was almost twice that of muscles from untreated mice (**Fig. 1d** and **Supplementary Figure 4** online). Frequency histograms of single-fiber area showed different size distributions in muscles from TSA-treated versus untreated mice, with a shift toward larger areas consistently observed in muscles from TSA-treated mice (**Supplementary Figure 4**). Notably, TSA treatment preserved the normal muscle architecture, which is typically subverted in dystrophic mice as the disease progresses (**Fig. 1d**).

The frequency of centrally nucleated fibers (data not shown) and the number of cell expressing the satellite activation marker desmin progressively declined with the duration of TSA exposure (**Supplementary Figure 5** online). Satellite cells are activated in response to contraction-coupled degeneration; hence, the reduced number of satellite cells in treated animals is likely to reflect the decreased susceptibility of dystrophic muscles, enlarged in response to TSA, to the cycles of degeneration and regeneration induced by contraction.

Typical histological features of dystrophic muscles include abundant inflammatory infiltrate and fibrosis, which lead to the progressive replacement of myofibers with connective tissue. Azan Mallory staining revealed frequent foci of fibrosis in muscles of untreated 6-month-old MDX mice, as reflected by the increased presence of hydroxyproline. TSA treatment eliminated fibrosis and cellular infiltrate in all muscles analyzed. This effect was accompanied by a drastic reduction in muscle necrosis, which reflects sarcolemma stability and was monitored *in vivo* by Evans blue uptake (**Supplementary Figure 6** online).

MDX mice share with α-SG–deficient mice—a model of limb girdle muscular dystrophy (LGMD)[11]—several pathogenic features, including sarcolemma instability due to disruption of the dystrophin-glycoprotein complex that is caused by the mutation of dystrophin (in MDX mice) or α-SG (in α-SG–deficient mice). Myostatin blockade at early stages of the disease provides a beneficial effect in both MDX and α-SG–deficient mice[4,5,12]. These functional analogies led us to think that the beneficial effect of TSA that we observed in MDX mice might be extended to α-SG–deficient mice. Prolonged delivery of TSA in α-SG–deficient mice promoted satellite-mediated formation of hypernucleated myotubes *in vitro* (**Supplementary Figure 7** online), increased their muscle size and reduced both fibrosis (**Supplementary Figure 7**) and cellular infiltrate *in vivo* (data not shown).

Deacetylase inhibitor–mediated upregulation of follistatin in myoblasts is an essential event in promoting the formation of hypernucleated myotubes, and is correlated with an increased regeneration of injured muscles in normal mice exposed to deacetylase inhibitors[8]. Accordingly, follistatin RNA and protein levels were selectively increased in muscles from TSA-treated MDX mice (**Fig. 2a**,**b**). To establish a causal relationship between follistatin induction and the ability of TSA to promote the formation of muscles with an increased size, we reduced follistatin levels in freshly isolated myofibers by retrovirus-mediated RNA interference (RNAi). As retroviral infection selectively targets dividing cells, we assumed that only the nuclei of activated satellite cells were infected. Myofibers derived from TSA-treated MDX mice gave rise to satellite cells that showed an increased expression of follistatin and embryonic MyHC (**Fig. 2c**) and formed multinucleated myotubes earlier and with an increased size (**Fig. 2d**), as compared to myofibers from untreated MDX mice. RNAi-mediated reduction of follistatin in satellite cells from myofibers of TSA-treated MDX mice eliminated their ability to respond to TSA (**Fig. 2c**,**d**), indicating that the increased size of muscles of TSA-treated MDX mice relies on follistatin upregulation in satellite cells. The proximal promoter region of follistatin, containing MyoD-, CREB- and NFAT-responsive elements, regulates muscle-restricted expression

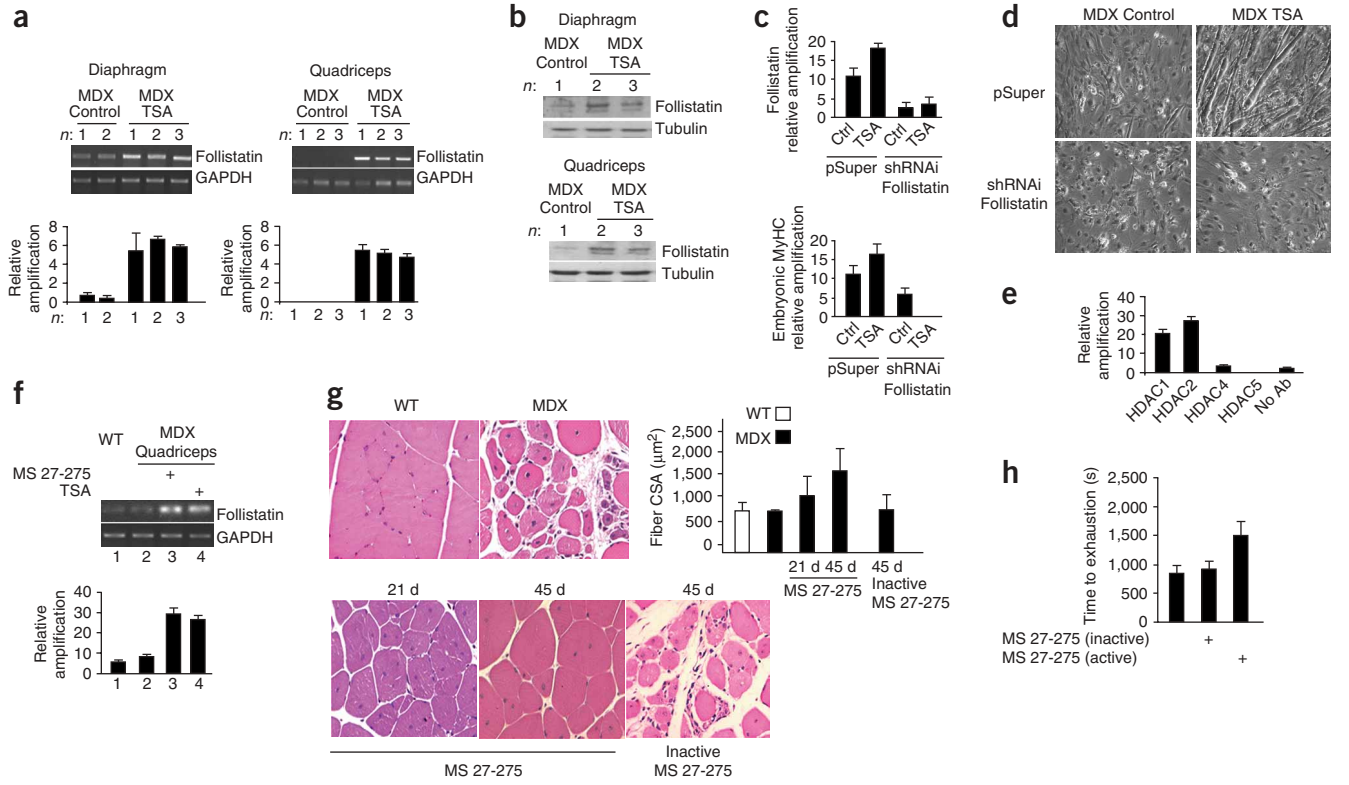

Figure 2 Induction of follistatin mediates the increased efficiency of myotube formation from satellite cells derived by myofibers of dystrophic muscles. (**a**,**b**) Expression of follistatin transcripts and protein in whole diaphragm and quadriceps isolated from MDX mice treated (TSA) or not treated (control) with TSA for 21 d, by RT-PCR (**a**, top) and real-time PCR (**a**, bottom) or western blot (**b**). (**c**,**d**) Single myofibers isolated from untreated (ctrl) or TSA-treated MDX mice and infected with retroviruses encoding either follistatin short hairpin RNAi (shRNAi) or pSuper vector. Two days after the infection, colonies of released satellite cells were expanded and placed in differentiation medium. Expression of follistatin and embryonic MyHC was evaluated by real-time PCR (**c**) and myotube formation was scored by evaluating the percentage per field of nuclei in multinucleated myotubes/total nuclei (fusion index) (**d**): MDX control pSuper, <5%; MDX control shRNAi follistatin, <5%; MDX + TSA, 75.4%; MDX + TSA shRNAi follistatin, <5%. (**e**) Chromatin immunoprecipitation analysis of chromatin isolated from C2C12 myoblasts to detect the relative abundances of HDAC1, HDAC2, HDAC4 and HDAC5 on the –500 bp region of the follistatin promoter. No Ab, control without antibody. (**f**) Expression of follistatin transcripts in whole quadriceps isolated from WT and MDX mice not treated or treated for 21 d with TSA or MS 27-275, monitored by RT-PCR (top) and real-time PCR (bottom). (**g**) H&E staining of quadriceps from MDX mice not treated or treated with MS 27-275 (either the active or inactive isomer) for 21 or 45 d to evaluate the distribution of CSA (untreated versus treated 45 d $P < 0.001$; $n = 4$). Original magnification, ×40. (**h**) Exercise performance evaluated by treadmill test in 12-week-old MDX mice not treated or treated with MS 27-275 (either the active or inactive isomer). MS 27-275–treated mice displayed a performance significantly higher than MDX mice at 45 d (MDX inactive versus active isomer treated $P < 0.01$, $n = 6$).

of follistatin[8]. Selective association of MyoD and CREB with class I histone deacetylases (HDACs) represses downstream gene transcription[13,14], and only the class I HDACs HDAC1 and HDAC2 occupied the chromatin of the proximal follistatin promoter in myoblasts (**Fig. 2e**). We sought to narrow down the target of the pharmacological activity of deacetylase inhibitors in muscles by comparing the effect of the benzamide derivative MS 27-275, which selectively inhibits class I HDACs (**Supplementary Figure 8** online)[15], with that of TSA, which indiscriminately inhibits class I and II deacetylases. As a control, we used the inactive isomer of MS 27-275. Treatment of MDX mice with MS 27-275 upregulated follistatin expression in muscles (**Fig. 2f**), increased the fiber CSA (**Fig. 2g**) and reduced both muscle fibrosis and cellular infiltrate (**Supplementary Figure 8**), leading to a full recovery of exercise performance (**Fig. 2h**). These data indicate that selective inhibition of class I deacetylases can replicate the beneficial effects of TSA in MDX mice.

The effectiveness of deacetylase inhibitors in the experimental therapy of mouse models of muscular dystrophy is of particular pharmacological interest, given the availability of these compounds for trials in human diseases. Although the results presented here should encourage preclinical studies to evaluate the potential beneficial effects of deacetylase inhibitors in the pharmacological therapy of muscular dystrophy, it will be important to further elucidate their mechanism of action in order to identify more selective strategies to counter the progression of the disease.

The procedures and experiments on mice described in this manuscript were approved by the Ministry of the Health of Italy (Decreto n 122/2003-A); official document available upon request.

Note: Supplementary information is available on the Nature Medicine website.

ACKNOWLEDGMENTS

We thank K.P. Campbell (Howard Hughes Medical Institute, University of Iowa) for providing α-SG–deficient mice, G. Cossu. and E. Engvall for critically reading the manuscript, and Alberto Bordonaro for the art work on figures. P.L.P is an assistant Telethon scientist at the Dulbecco Telethon Institute. This work was supported by a Telethon Special Grant to P.L.P. and R.B.; Muscular Dystrophy Association, Parent Project Organization and Compagnia San Paolo di Torino grants to P.L.P.; a European Union Grant and a Telethon Grant to M.C.C.; an Associazione Italiana Ricerca sul Cancro Regional Grant to C.G.; Cariplo

Foundation and Italian Space Agency grants to R.B.; and grants from the Intramural Research Program of the National Institute of Arthritis and Musculoskeletal and Skin Diseases of the US National Institutes of Health to M.D.P and V.S.

COMPETING INTERESTS STATEMENT

The authors declare competing financial interests (see the *Nature Medicine* website for details).

Published online at http://www.nature.com/naturemedicine
Reprints and permissions information is available online at http://npg.nature.com/reprintsandpermissions/

1. Engvall, E. & Wewer, U.M. *FASEB J.* **17**, 1579–1584 (2003).
2. Zammit, P.S. & Partridge, T.A. *Nat. Med.* **8**, 1355–1356 (2002).
3. Lee, S.J. *Annu. Rev. Cell Dev. Biol.* **20**, 61–86 (2004).
4. Bogdanovich, S. *et al. Nature* **420**, 418–421 (2002).
5. Wagner, K.R., McPherron, A.C., Winik, N. & Lee, S.J. *Ann. Neurol.* **52**, 832–836 (2002).
6. Barton, E.R., Morris, L., Musaro, A., Rosenthal, N. & Sweeney, H.L. *J. Cell Biol.* **157**, 137–148 (2002).
7. Iezzi, S., Cossu, G., Nervi, C., Sartorelli, V. & Puri, P.L. *Proc. Natl. Acad. Sci. USA* **99**, 7757–7762 (2002).
8. Iezzi, S. *et al. Dev. Cell* **6**, 673–684 (2004).
9. Emery, A.E. *Lancet* **359**, 687–695 (2002).
10. Rafael, J.A., Tinsley, J.M., Potter, A.C., Deconinck, A.E. & Davies, K.E. *Nat. Genet.* **19**, 79–82 (1998).
11. Duclos, F. *et al. J. Cell Biol.* **142**, 1461–1471 (1998).
12. Parsons, S.A., Millay, D.P., Sargent, M.A., McNally, E.M. & Molkentin, J.D. *Am. J. Pathol.* **168**, 1975–1985 (2006).
13. Puri, P.L. *et al. Mol. Cell* **8**, 885–897 (2001).
14. Canettieri, G. *et al. Nat. Struct. Biol.* **10**, 175–181 (2003).
15. Saito, A. *et al. Proc. Natl. Acad. Sci. USA* **96**, 4592–4597 (1999).